Pergamon

Available online at www.sciencedirect.com

SCIENCE DIRECT®

Cement and Concrete Research 34 (2004) 1893–1897

CEMENT AND CONCRETE RESEARCH

Microstructural effect of the shrinkage of cement-based materials during hydration, as indicated by electrical resistivity measurement

Jingyao Cao, D.D.L. Chung*

Composite Materials Research Laboratory, University at Buffalo, State University of New York, Furnas Hall Room 608, Buffalo, NY 14260-4400, USA

Received 12 December 2002; accepted 2 February 2004

Abstract

The effect of shrinkage during hydration on the microstructural change in cement-based materials was studied by measuring electrical resistivity and shrinkage strain. The microstructural change caused by shrinkage, as indicated by the fractional change in resistivity at the same shrinkage strain, is diminished with silica fume and increased with sand. The resistivity abruptly and irreversibly increases at a shrinkage strain of 3×10^{-4}. The increase is negligible when silica fume is present. The fractional change in resistivity per unit shrinkage strain is much larger than the fractional change in resistivity per unit compressive strain in the cured state.

Keywords: Electrical properties; Physical properties; Shrinkage; Silica fume; Microstructure

1. Introduction

The hydration reaction that occurs during the curing of cement causes shrinkage, called autogenous shrinkage, which is accompanied by a decrease in the relative humidity within the pores. In case that the curing is conducted in an open atmosphere, shrinkage called drying shrinkage occurs due to the movement of water through the pores to the surface and the loss of water on the surface by evaporation. The total shrinkage is the quantity addressed in this article, as it is practically important.

The shrinkage of cement-based materials during hydration is a cause of defects (such as cracks) in cement-based materials. It can also cause prestressing loss [1]. The tendency for defect formation during shrinkage increases with increasing size of the cement-based material.

The effects of shrinkage have been studied by numerous workers by measurement of the shrinkage strain and observation of the cracks. However, the microstructural change, which necessarily proceeds the cracking, has not been studied. The extent of microstructural change and the evolution of the microstructure as shrinkage occurs are important for the understanding of the shrinkage process. This understanding is valuable for the alleviation of the problem associated with shrinkage-induced cracking.

A nondestructive technique that is sensitive to the microstructure is appropriate for monitoring the microstructural effect of shrinkage. One such technique is electrical resistivity measurement. Microscopy is sensitive to the microstructure, but it is tedious and is not suitable for real-time observation. This work thus uses resistivity measurement to monitor the microstructural effect of shrinkage. Resistivity measurement has been previously used to monitor mechanical deformation and damage [2], freeze–thaw cycling [3], and cementitious bond degradation [4], but has not been previously used to monitor shrinkage, whether drying or autogenous shrinkage.

Silica fume [5–8] is very fine noncrystalline silica produced by electric arc furnaces as a by-product of the production of metallic silicon or ferrosilicon alloys. It is powder with particles having a diameter 100 times smaller than the anhydrous Portland cement particles. The SiO_2 content ranges from 85% to 98%. Silica fume used as an admixture in a concrete mix has significant effect on the properties of the resulting material [9].

The addition of untreated silica fume to cement paste decreases the drying shrinkage [1,10–15]. This desirable effect is partly due to the reduction of the pore size and connectivity of the voids and partly due to the prestressing

---

* Corresponding author. Tel.: +1-716-645-2593x2243; fax: +1-716-645-3875.

E-mail address: ddlchung@buffalo.edu (D.D.L. Chung).

0008-8846/$ – see front matter © 2004 Elsevier Ltd. All rights reserved.
doi:10.1016/j.cemconres.2004.02.002

effect of silica fume, which restrains the shrinkage. The use of silane-treated silica fume in place of untreated silica fume further decreases the drying shrinkage, due to the hydrophylic character of the silane-treated silica fume and the formation of chemical bonds between silica fume particles and cement [10]. The use of silane and untreated silica fume as two admixtures also decreases the drying shrinkage, but not as significantly as the use of silane-treated silica fume [10]. However, silica fume has also been reported to increase the drying shrinkage [11,16,17] and the restrained shrinkage crack width is increased by silica fume addition [18]. This is partly because of the dependence of the silica fume effect on the water/cement ratio.

Due to the pozzolanic nature of silica fume, silica fume addition increases the autogenous shrinkage, as well as the autogenous relative humidity change [19,20]. These effects are undesirable, as they may cause cracking if the deformation is restrained. Aggregates are known to decrease the drying shrinkage [21]. However, the effect of aggregates on the microstructural evolution during drying shrinkage has not been previously addressed.

To investigate the effect of silica fume and fine aggregate on the shrinkage-induced microstructural change, this article addresses the drying shrinkage of cement pastes with and without silica fume (untreated) and of mortar without silica fume. Both the shrinkage strain and the electrical resistivity (obtained from the electrical resistance and the strain) were measured continually from 1 to 28 days of curing.

2. Experimental methods

The cement used was Portland cement (Type I) from Lafarge (Southfield, MI). The silica fume (Elkem Materials, Pittsburgh, PA, microsilica EMS 965) was used at 15% by mass of cement [9]. Four types of cement paste were studied, namely, (a) plain cement paste (consisting of just cement and water) with a water/cement ratio of 0.30, (b) plain cement paste with a water/cement ratio of 0.35, (c) plain cement paste with a water/cement ratio of 0.40, and (d) silica fume cement paste with a water/cement ratio of 0.35. A water-reducing agent (WR) was used at 1.5%, 1.0%, 1.0%, and 2.0% by mass of cement for cement pastes (a), (b), (c), and (d), respectively. The WR was TAMOL SN (Rohm and Haas, Philadelphia, PA), which contained 93–96% sodium salt of a condensed naphthalene sulfonic acid.

One type of mortar [labeled (e)] was studied. It was plain mortar with a water/cement ratio of 0.35. The sand used in the mortar was natural sand (100% passing 2.36-mm sieve, 99.9% SiO_2). The sand/cement ratio was 1.0. For the mortar, WR was used in the amount of 1.0% by weight of cement.

A rotary mixer with a flat beater was used for mixing. Cement, water, silica fume (if applicable), and sand (if applicable) were mixed in the mixer for 5 min. After pouring the mix into oiled molds, an external electric vibrator was used to facilitate compaction. The specimens were demolded after 1 day and then allowed to cure at room temperature in air (relative humidity = 100%) for 28 days.

Six specimens of each composition were tested by monitoring simultaneously the shrinkage and the volume electrical resistivity in the same direction as the shrinkage, daily during 28 days of curing. Each data point reported here was the average value for the six specimens.

Shrinkage measurement was conducted on specimens of size 280 × 25.4 × 25.4 mm. A stainless steel contact point was positioned at each end along the length of each sample, such that the exterior tips of the two contact points were outside the sample and the interior tips of the two contact points were inside the sample and were separated by a distance of 250 mm, which was the gage length for shrinkage strain measurement (Fig. 1). The measurement was conducted in accordance with ASTM Method C490-93a.

During shrinkage testing, the resistivity was measured using the four-probe method [22], except that the two-probe method was used in case of the mortar at 11 days and beyond, due to the high resistance involved. Silver paint in conjunction with copper wires served as electrical contacts. Four contacts were perimetrically around the specimen at four planes that were all perpendicular to the strain axis and that were symmetric with respect to the midpoint along the height of the specimen (Fig. 1). The outer two contacts (typically 270 mm apart) were for passing current. The inner two contacts (typically 260 mm apart) were for measuring the voltage. A Keithley 2001 multimeter was used. In the case of the two-probe method, only the inner contacts were used. Thus, the gage length for resistivity measurement was the distance be-

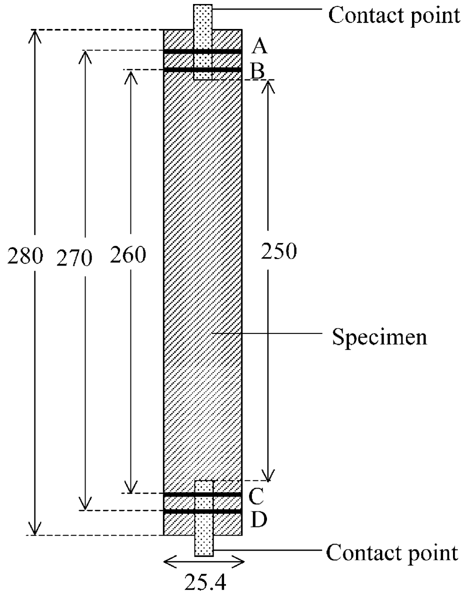

Fig. 1. Specimen configuration for measurement of shrinkage and electrical resistivity in the direction of the shrinkage. A and D are for passing current; B and C are for voltage measurement. All dimensions are in millimeters.

Table 1
Volume electrical resistivity and resistance at 1 day of curing

Material	Resistivity (Ω cm)	Resistance (MΩ)	Water/cement ratio
(a)	1.01×10^6	0.233	0.30
(b)	1.06×10^6	0.244	0.35
(c)	1.11×10^6	0.257	0.40
(d)[a]	5.46×10^5	0.126	0.35
(e)[b]	1.56×10^7	3.59	0.35

[a] With silica fume.

[b] With sand.

tween B and C in Fig. 1. The steel contact points have negligible effect on the fractional change in measured resistivity of the specimen during hydration.

The resistivity was obtained from the resistance and the dimensions (both the length in the current direction and the cross-sectional area perpendicular to the current direction), which changed with the measured longitudinal strain and with the transverse strain resulting from the Poisson effect. However, neglecting the transverse strain affected the longitudinal resistivity value negligibly. The fractional change in resistance was essentially equal to the fractional change in resistivity.

3. Results and discussion

Table 1 shows the initial (1 day of curing) values of the volume electrical resistivity and resistance for each of the five compositions investigated. The resistivity increased with increasing water/cement ratio. It was decreased by the addition of silica fume and was increased by the addition of sand. The resistivity was not measured prior to 1 day of curing because of the need to apply electrical contacts on a specimen after demolding.

Figs. 2 and 3 show the shrinkage strain and fractional change in resistivity, respectively, vs. curing age. The presence of silica fume decreases both the shrinkage strain and fractional change in resistivity at the same curing age between 1 and 28 days. This means that the silica fume restrains the shrinkage as well as the shrinkage-induced microstructural change. Both shrinkage strain and fractional change in resistivity increase smoothly with increasing curing age, such that the increase becomes more gradual as curing progresses.

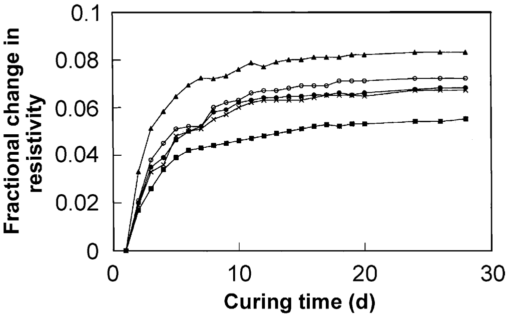

Fig. 3. Fractional change in resistivity vs. curing time for plain cement paste with water/cement ratio = 0.30 (×), plain cement paste with water/cement ratio = 0.35 (●), plain cement paste with water/cement ratio = 0.40 (○), silica fume cement paste (■), and plain mortar (▲).

Sand decreases the shrinkage strain even more than silica fume (Fig. 2), but the fractional change in resistivity is increased by sand. This means that the shrinkage-induced microstructural change is larger when sand is present, presumably due to the effect of shrinkage on the microstructure of the interface between sand and cement. Sand does not shrink while cement shrinks, thereby resulting in microstructural change at the sand–cement interface as drying shrinkage proceeds. The interface is associated with a contact electrical resistance, which increases as the interfacial voids or void precursors become more numerous. The increase of the contact resistivity between steel rebar and concrete as shrinkage proceeds has been previously reported [23].

An increase in the water/cement ratio causes a negligible increase in the shrinkage strain (Fig. 2) but a slight increase in the fractional change in resistivity (Fig. 3). This means that the shrinkage-induced microstructural change increases

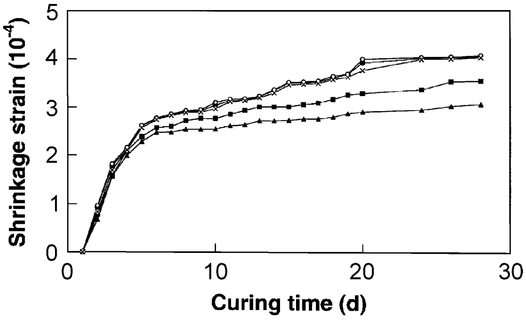

Fig. 2. Shrinkage strain vs. curing time for plain cement paste with water/cement ratio = 0.30 (×), plain cement paste with water/cement ratio = 0.35 (●), plain cement paste with water/cement ratio = 0.40 (○), silica fume cement paste (■), and plain mortar (▲).

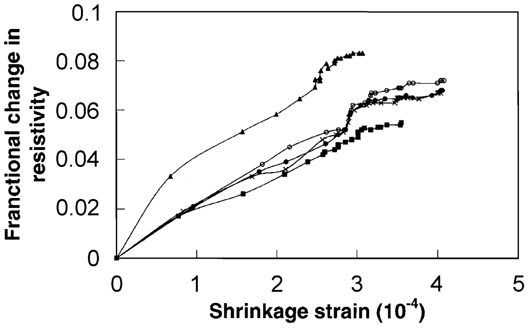

Fig. 4. Fractional change in resistivity vs. shrinkage strain for plain cement paste with water/cement ratio = 0.30 (×), plain cement paste with water/cement ratio = 0.35 (●), plain cement paste with water/cement ratio = 0.40 (○), silica fume cement paste (■), and plain mortar (▲).

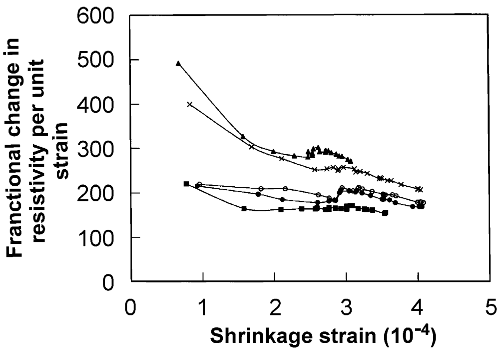

Fig. 5. Fractional change in resistivity per unit strain vs. shrinkage strain for plain cement paste with water/cement ratio = 0.30 (×), plain cement paste with water/cement ratio = 0.35 (●), plain cement paste with water/cement ratio = 0.40 (○), silica fume cement paste (■), and plain mortar (▲).

slightly with increasing water/cement ratio. The effect of the water/cement ratio is much smaller than that of silica fume or sand. However, the use of data at 1 day of curing as the reference values for the study of the fractional change upon hydration is not ideal, due to the degree of hydration being not the same at 1 day of curing for the different water/cement ratios.

Fig. 4 shows that the fractional change in resistivity is less in the presence of silica fume for the same strain. This implies that the extent of microstructural change at the same strain is less in the presence of silica fume. Fig. 4 also shows that the fractional change in resistivity is higher in the presence of sand for the same strain. Thus, the extent of microstructural change at the same strain is more in the presence of sand.

Fig. 4 shows that the fractional change in resistivity abruptly increases at a strain of 3.0×10^{-4} for all cement pastes without silica fume and at a strain of 2.5×10^{-4} for mortar. This abrupt resistivity increase is probably associated with an abrupt and irreversible microstructural change. The addition of silica fume essentially eliminates this effect, whereas the addition of sand causes the microstructural change to occur at a lower shrinkage strain. This is consistent with the notion that silica fume addition diminishes the shrinkage-induced microstructural change, whereas sand addition increases this quantity.

Fig. 5 shows that the fractional change in resistivity per unit strain is in the range 150–500. This quantity describes the severity of shrinkage-induced microstructural change. The severity is slightly lower in the presence of silica fume, and is significantly higher in the presence of sand. The severity tends to decrease as shrinkage proceeds, as expected from the decreasing rate of shrinkage as shrinkage proceeds (Fig. 2).

The fractional change in resistivity per unit compressive strain in the cured state, as determined during compressive loading, is 10 [2]. Thus, the microstructural change induced by shrinkage strain is much larger than that induced by compressive strain for the same amount of strain. Nevertheless, both shrinkage strain and compressive strain cause the resistivity in the strain direction to increase. The large microstructural change during shrinkage is expected from the hydration reaction, which takes place during curing.

The microstructural changes mentioned in this article may relate to the changes in the interfacial microstructure, as suggested by the relatively large microstructural change in the presence of sand. They may also relate to the nonuniformity in the distribution of moisture, including free water and water in the hydrate. This nonuniformity is probably diminished by silica fume, as suggested by the relatively small microstructural change in the presence of silica fume.

4. Conclusions

1. The microstructural change induced in cement by shrinkage during hydration is diminished by the addition of silica fume and is increased by the addition of sand, as shown by the fractional change in electrical resistivity (relative to the value at 1 day of curing) at the same shrinkage strain. An increase in the water/cement ratio from 0.30 to 0.40 increases this quantity slightly. The effect of the water/cement ratio is small compared to those of silica fume and sand.
2. The fractional change in resistivity (indicating the extent of shrinkage-induced microstructural change) abruptly and irreversibly increases at a shrinkage strain of 3.0×10^{-4} in all cement pastes, except that the effect is essentially absent when silica fume is present. In the case of mortar, the abrupt and irreversible increase occurs at a lower shrinkage strain of 2.5×10^{-4}.
3. The fractional change in resistivity per unit shrinkage strain ranges from 150 to 500, which is much larger than the fractional change in resistivity per unit compressive strain in the cured state. This quantity is increased by the addition of sand and is decreased by the addition of silica fume.

References

[1] V. Baroghel-Bouny, J. Godin, New experimental approach to drying shrinkage in ordinary and very high performance paste and hardened concrete, Bull. Liaison Lab. Ponts Chaussées 218 (1998) 39–48.
[2] J. Cao, S. Wen, D.D.L. Chung, Defect dynamics and damage of cement-based materials, studied by electrical resistance measurement, J. Mater. Sci. 36 (18) (2001) 4351–4360.
[3] J. Cao, D.D.L. Chung, Damage evolution during freeze–thaw cycling of cement mortar, studied by electrical resistivity measurement, Cem. Concr. Res. 32 (10) (2002) 1657–1661.
[4] J. Cao, D.D.L. Chung, Cementitious bond degradation during cyclic shear loading, studied by contact electrical resistance measurement, J. Mater. Sci. 36 (18) (2001) 4345–4349.
[5] M.D. Luther, P.A. Smith, Silica fume (microsilica) fundamentals for use in concrete, Proc. Eng. Found. Conf. (1991) 75–106.
[6] V.M. Malhotra, Fly ash, slag, silica fume, and rice-husk ash in concrete. A review, Concr. Int.: Des. Constr. 15 (4) (1993) 23–28.
[7] M.D. Luther, Silica fume (microsilica) concrete in bridges, Concr. Int.: Des. Constr. 15 (4) (1993) 29–33.

[8] J. Wolsiefer, D.R. Morgan, Silica fume in shotcrete, Concr. Int.: Des. Constr. 15 (4) (1993) 34–39.

[9] D.D.L. Chung, Improving cement-based materials by using silica fume, J. Mater. Sci. 27 (4) (2002) 673–682.

[10] Y. Xu, D.D.L. Chung, Improving silica fume cement by using silane, Cem. Concr. Res. 30 (8) (2000) 1305–1311.

[11] M.N. Haque, Strength development and drying shrinkage of high-strength concretes, Com. Concr. Compos. 18 (5) (1996) 333–342.

[12] S.H. Alsayed, Influence of superplasticizer, plasticizer, and silica fume on the drying shrinkage of high-strength concrete subjected to hot–dry field conditions, Cem. Concr. Res. 28 (10) (1998) 1405–1415.

[13] A. Lamontagne, M. Pigeon, R. Pleau, D. Beaupre, Use of air-entraining admixtures in dry-mix shotcrete, ACI Mater. J. 93 (1) (1996) 69–74.

[14] M.G. Alexander, Deformation properties of blended cement concretes containing blastfurnace slag and condensed silica fume, Adv. Cem. Res. 6 (22) (1994) 73–81.

[15] F.H. Al-Sugair, Analysis of the time-dependent volume reduction of concrete containing silica fume, Mag. Concr. Res. 47 (170) (1995) 77–81.

[16] B. Bissonnette, M. Pigeon, Tensile creep at early ages of ordinary, silica fume and fiber reinforced concretes, Cem. Concr. Res. 25 (5) (1995) 1075–1085.

[17] G.A. Rao, Influence of silica fume replacement of cement on expansion and drying shrinkage, Cem. Concr. Res. 28 (10) (1998) 1505–1509.

[18] Z. Li, M. Qi, Z. Li, B. Ma, Crack width of high-performance concrete due to restrained shrinkage, J. Mater. Civ. Eng. 11 (3) (1999) 214–223.

[19] O.M. Jensen, P.F. Hansen, Autogenous deformation and change of the relative humidity in silica fume-modified cement paste, ACI Mater. J. 93 (6) (1996) 539–543.

[20] O.M. Jensen, P.F. Hansen, Autogenous relative humidity change in silica fume-modified cement paste, Adv. Cem. Res. 7 (25) (1995) 33–38.

[21] P.-W. Chen, D.D.L. Chung, Concrete reinforced with up to 0.2 vol.% of short carbon fibers, Composites 24 (1) (1993) 33–52.

[22] D.D.L. Chung, Applied Materials Science, CRC Press, Boca Raton. Florida, 2002 (Appendix C).

[23] D.D.L. Chung, Interface engineering for cement–matrix composites, Compos. Interfaces 8 (1) (2001) 67–82.